Obesity challenges the hepatoprotective function of the integrated stress response to asparaginase exposure in mice

Received for publication, November 18, 2016, and in revised form, February 17, 2017 Published, Papers in Press, February 27, 2017, DOI 10.1074/jbc.M116.768408

Inna A. Nikonorova[‡1], Rana J. T. Al-Baghdadi[§2], Emily T. Mirek[‡], Yongping Wang[‡], Michael P. Goudie[‡], Berish B. Wetstein[‡], Joseph L. Dixon[‡¶], Christopher Hine[‖], James R. Mitchell[‖], Christopher M. Adams[**], Ronald C. Wek[‡‡], and Tracy G. Anthony[‡§¶3]

From the [‡]Department of Nutritional Sciences, and the [§]Endocrinology and Animal Biosciences Graduate Program, Rutgers, The State University of New Jersey, New Brunswick, New Jersey 08901, the [¶]Rutgers Center for Lipid Research, New Jersey Institute for Food, Nutrition and Health, New Brunswick, New Jersey 08901, the [‖]Department of Genetics and Complex Diseases, Harvard T.H. Chan School of Public Health, Boston, Massachusetts 02115, the [**]Department of Internal Medicine, Roy J. and Lucille A. Carver College of Medicine, University of Iowa, Iowa City, Iowa 52242, and the [‡‡]Department of Biochemistry and Molecular Biology, Indiana University, School of Medicine, Indianapolis, Indiana 46202

Edited by Jeffrey E. Pessin

Obesity increases risk for liver toxicity by the anti-leukemic agent asparaginase, but the mechanism is unknown. Asparaginase activates the integrated stress response (ISR) via sensing amino acid depletion by the eukaryotic initiation factor 2 (eIF2) kinase GCN2. The goal of this work was to discern the impact of obesity, alone *versus* alongside genetic disruption of the ISR, on mechanisms of liver protection during chronic asparaginase exposure in mice. Following diet-induced obesity, biochemical analysis of livers revealed that asparaginase provoked hepatic steatosis that coincided with activation of another eIF2 kinase PKR-like endoplasmic reticulum kinase (PERK), a major ISR transducer to ER stress. Genetic loss of *Gcn2* intensified hepatic PERK activation to asparaginase, yet surprisingly, mRNA levels of key ISR gene targets such as *Atf5* and *Trib3* failed to increase. Instead, mechanistic target of rapamycin complex 1 (mTORC1) signal transduction was unleashed, and this coincided with liver dysfunction reflected by a failure to maintain hydrogen sulfide production or apolipoprotein B100 (ApoB100) expression. In contrast, obese mice lacking hepatic activating transcription factor 4 (*Atf4*) showed an exaggerated ISR and greater loss of endogenous hydrogen sulfide but normal inhibition of mTORC1 and maintenance of ApoB100 during asparaginase exposure. In both genetic mouse models, expression and phosphorylation of Sestrin2, an ATF4 gene target, was increased by asparaginase, suggesting mTORC1 inhibition during asparaginase exposure is not driven via eIF2-ATF4-Sestrin2. In conclusion, obesity promotes a maladaptive ISR during asparaginase exposure. GCN2 functions to repress mTORC1 activity and maintain ApoB100 protein levels independently of *Atf4* expression, whereas hydrogen sulfide production is promoted via GCN2-ATF4 pathway.

Asparaginase (ASNase)[4] is an important drug in the treatment of acute lymphoblastic leukemia in children and adults. It functions by depleting circulating asparagine and glutamine, essential for the growth of the leukemic lymphoblast (1). Despite decades of clinical use, medical professionals remain uncertain how to predict and/or prevent a range of asparaginase-triggered metabolic toxicities that lead to treatment failure (2, 3). Furthermore, the risk of asparaginase-associated non-hematologic adverse events such as hepatotoxicity is significantly greater in obese patients (4).

Asparaginase treatment is a form of amino acid stress that increases phosphorylation of eukaryotic initiation factor 2 (eIF2) in liver and other tissues by general control nonderepressible kinase 2 (GCN2; EIF2AK4 in humans) (5, 6). GCN2 is one of four eIF2 kinases that collectively activate a homeostatic program coined the integrated stress response (ISR) under a variety of stress conditions, including amino acid depletion. A second eIF2 kinase, protein kinase R-like endoplasmic reticulum kinase (PERK; EIF2AK3 in humans) is localized to the ER and is activated upon stress in this organelle. Activation of the integrated stress response via phosphorylation of eIF2 attenuates global protein synthesis in favor of gene-specific mRNA

This work was supported, in whole or in part, by National Institutes of Health Grants RO1HD070487 (to T. G. A.), K99AG050777 (to C. H.), and AR059115 (to C. M. A.) and Veterans Affairs Grants BX00976 and RX001477 (to C. M. A.). The authors declare that they have no conflicts of interest with the contents of this article. The content is solely the responsibility of the authors and does not necessarily represent the official views of the National Institutes of Health.

This article contains supplemental Figs. S1–S5.

[1] Supported by IRACDA New Jersey-New York for Science Partnerships in Research and Education National Institutes of Health postdoctoral training Grant K12GM093854.

[2] Supported via The Higher Committee for Education Development in Iraq (HCED) fellowship. Present address: Dept. of Physiology and Pharmacology, College of Veterinary Medicine, University of Al-Qadisiyah, Iraq.

[3] To whom correspondence should be addressed: 59 Dudley Rd., New Brunswick, NJ 08901. Tel.: 848-932-6331; Fax: 732-932-6837; E-mail: tracy.anthony@rutgers.edu.

[4] The abbreviations used are: ASNase, asparaginase; ISR, integrated stress response; GCN2, general control nonderepressible 2; mTORC1, mechanistic target of rapamycin complex 1; ATF4, activating transcription factor 4; PERK, protein kinase R-like endoplasmic reticulum kinase; CHOP, CCAAT/enhancer-binding protein homologous protein; GADD34, growth arrest and DNA damage-inducible protein, also known as PPP1R15A, protein phosphatase 1 regulatory subunit 15A; ATF3, activating transcription factor 3; Asns, asparagine synthetase; ATF5, activating transcription factor 5; TRIB3, tribbles homolog 3; EPRS, glutamyl-prolyl-tRNA synthetase; S6K1, also known as p70S6k, ribosomal protein S6 kinase 1; 4E-BP1, eIF4E-binding protein 1; Akt, also known as PKB, protein kinase B; ER, endoplasmic reticulum; AMPK, AMP-activated protein kinase.

translation. The best characterized translationally-induced gene in the integrated stress response is activating transcription factor 4 (*Atf4*) (7), encoding a basic leucine zipper DNA-binding protein that dimerizes with itself and/or other basic leucine zipper transcription factors such as CCAAT/enhancer-binding protein homologous protein (CHOP, also known as DDIT3/GADD153) and ATF3 (8). The ATF4-directed transcriptional response to amino acid deprivation is homeostatic and self-limiting via induction of negative feedback regulators (9, 10). The duration and amplitude of ATF4 expression over time influences cellular decision making by dynamic mechanisms that are not well understood.

Previous work from our laboratory shows that deficiency in GCN2 predisposes to metabolic toxicities by asparaginase. Lean $Gcn2^{-/-}$ mice are normal and phenotypically indistinguishable from intact mice. However, when exposed to amino acid depletion by asparaginase, lean $Gcn2^{-/-}$ mice develop metabolic complications including hepatic dysfunction and injury, pancreatitis, and immunosuppression (6, 11–14). These findings are consistent with clinical reports identifying and associating specific single nucleotide polymorphisms in genes regulated by GCN2, such as *Asns* and *Atf5*, with poorer outcomes to asparaginase treatment (15, 16).

The objective of this investigation was to assess how metabolic and genetic determinants influence the hepatic ISR during asparaginase treatment. Herein, we report that diet-induced obesity promotes hepatic steatosis and stress during asparaginase. The level of hepatic stress created by asparaginase in obese mice was further intensified in the absence of GCN2, evidenced by premature morbidity that corresponded with inappropriate phosphorylation of PERK, hyperactivation of mechanistic target of rapamycin complex 1 (mTORC1) signaling, and a block in endogenous hydrogen sulfide production. Additional experiments revealed that loss of hepatic *Atf4* expression reduced hydrogen sulfide production but did not activate mTORC1 during asparaginase. These data support a model where ATF4 acts to transcriptionally limit ISR gene expression during amino acid depletion, whereas GCN2 functions to inhibit mTORC1 activity. These findings provide novel insights into how amino acid sensing pathways are altered by both metabolic state and genetic background, influencing the hepatoprotective capacity of the integrated stress response to amino acid depletion by asparaginase.

Results

Obesity promotes hepatic steatosis to asparaginase and hastens morbidity when in combination with Gcn2 deletion

To investigate the impact of diet-induced obesity on metabolic and molecular responses to asparaginase, $Gcn2^{+/+}$ wild type (WT) and $Gcn2^{-/-}$ mice were fed an obesogenic diet *ad libitum* for 12 weeks. Onset of obesity was monitored by body composition changes and development of glucose intolerance (Fig. 1, *A* and *B*, and supplemental Fig. S1, *A* and *B*). Overall fat accumulation was less in the $Gcn2^{-/-}$ cohort as compared with the WT strain, reaching statistical significance in the female group only. No differences in food intake were observed between the strains (supplemental Fig. S1*C*). Assessment of glucose tolerance showed that obese males of both strains differed significantly from their lean counterparts, whereas females were resistant to developing glucose intolerance. Furthermore, $Gcn2^{-/-}$ males cleared blood glucose slightly faster than WT mice regardless of body composition.

Following establishment of obesity, mice were assigned to once daily intraperitoneal injections of L-asparaginase or an equivolume of phosphate-buffered saline as a vehicle control. Asparaginase exposure promoted catabolism in all animals as evidenced by loss of body weight (Fig. 1*C*, and supplemental Fig. S2*A*), body fat and lean mass (supplemental Fig. S2*B*). Despite weight loss, all WT mice appeared healthy and active. In contrast, 5 of 13 $Gcn2^{-/-}$ animals (2 males and 3 females) developed metabolic distress prematurely and were euthanized after the 7th injection due to emerging morbidity. Hepatic gross morphology of harvested livers revealed an extreme accumulation of fat as evidenced by visually pale appearance (Fig. 1*D*), alongside increased liver size relative to body weight (supplemental Fig. S1*C*). Hepatic fat accumulation was also confirmed by triglyceride measurement (Fig. 1*E*). Abundance of hepatic apolipoprotein B triglyceride exporting protein (ApoB100) displayed a severe 5-fold reduction in asparaginase-treated $Gcn2^{-/-}$ mice only (Fig. 1*F*).

Although sex differences were observed in body composition and glucose tolerance to diet-induced obesity there was no sexual dimorphism in measured outcomes following asparaginase treatment. Therefore, results from males and females were combined in subsequent biochemical analyses.

Obesity activates PERK in livers of asparaginase-treated mice

Previously we identified GCN2 as the primary kinase activated by asparaginase in lean mice, and livers lacking GCN2 showed no eIF2 phosphorylation following 1, 6, or 8 daily injections (6, 11, 14). However, following onset of diet-induced obesity, asparaginase treatment robustly induced serine 51 phosphorylation of the α subunit of eIF2 (*p*-eIF2) in livers of WT and $Gcn2^{-/-}$ mice (Fig. 2*A*). To identify the source of *p*-eIF2 in $Gcn2^{-/-}$ mice we examined phosphorylation of PERK, a marker of its activation by ER stress (17). We found on average 20-fold increases in *p*-PERK in asparaginase-treated $Gcn2^{-/-}$ livers (Fig. 2*B*). WT mice treated with asparaginase also demonstrated significant hepatic phosphorylation of PERK (~5-fold increase over saline control), an effect not seen in lean mice and thus attributed to obese state.

To investigate the interrelationship between GCN2 and PERK-launched ISR in response to asparaginase-induced amino acid depletion we examined expression of ISR target genes. Transcript abundances of some genes (*e.g. Asns* and *Atf3*) were increased by asparaginase similarly in both strains, whereas other transcripts, tribbles homolog 3 (*Trib3*), *Atf5*, glutamyl-prolyl-tRNA synthetase (*Eprs*), and *Chop*, failed to be induced in livers of asparaginase-treated $Gcn2^{-/-}$ mice despite robust PERK phosphorylation (Fig. 2*C*). These results indicate that PERK activity cannot fully rescue activation of the ISR by GCN2 and are consistent with the report that the transcriptional signatures elicited by these two eIF2 kinases are distinct (18).

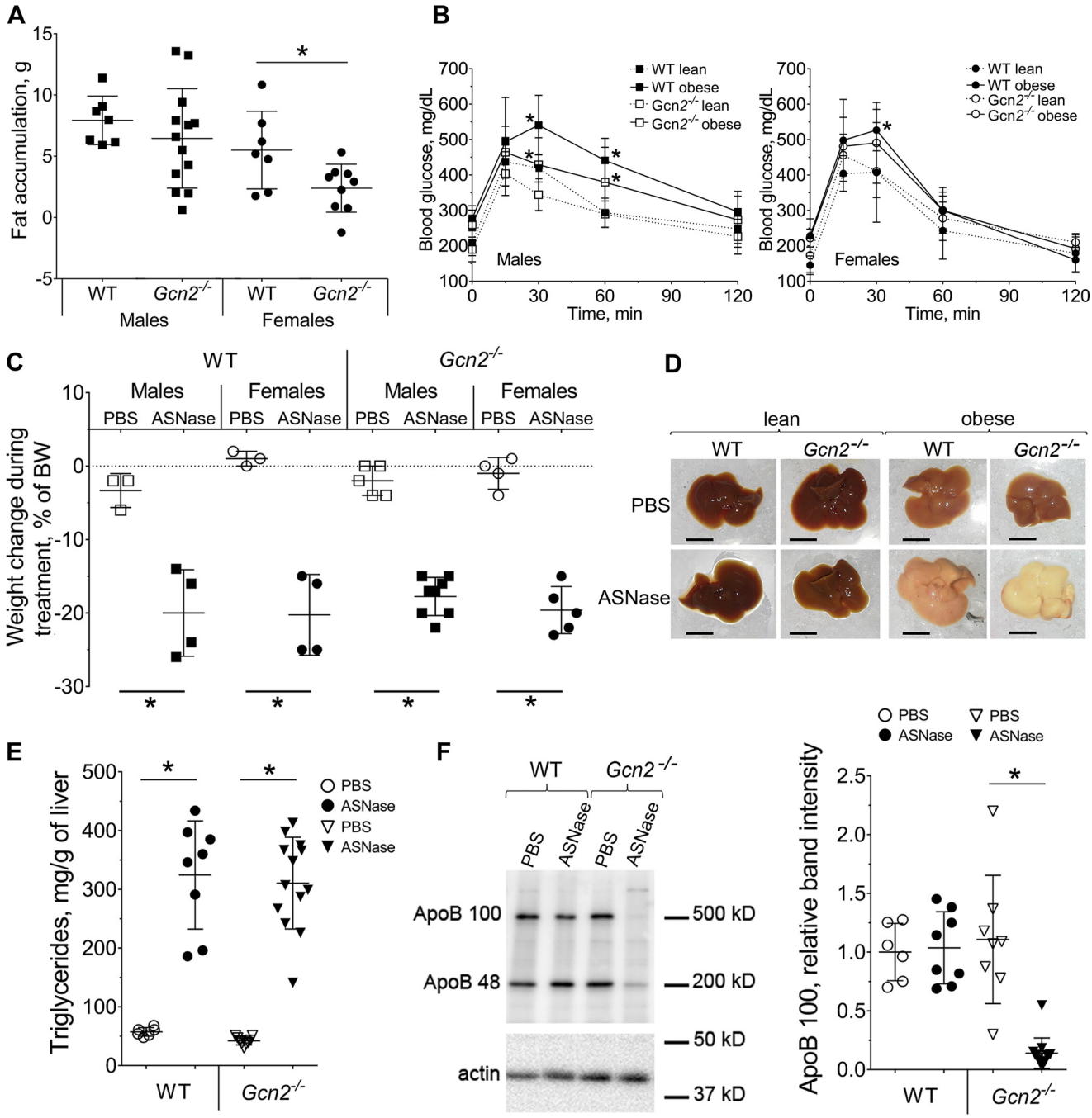

Figure 1. ASNase promotes liver steatosis in obese mice. *A*, body fat accumulation in male and female wild type (WT) and *Gcn2*$^{-/-}$ mice after 12 weeks of an obesogenic diet, assessed by magnetic resonance imaging. *B*, glucose clearance in male and female WT and *Gcn2*$^{-/-}$ mice after 12 weeks of an obesogenic diet. *C*, body weight change in male and female WT and *Gcn2*$^{-/-}$ mice following ASNase or PBS excipient, expressed as percent of starting body weight. *D*, gross morphology of livers from lean and obese WT and *Gcn2*$^{-/-}$ mice following ASNase or PBS. *Scale bar* is 1 cm. *E*, triglyceride accumulation in livers from obese WT and *Gcn2*$^{-/-}$ mice following ASNase or PBS. *F*, hepatic ApoB100 and ApoB48 protein abundance in WT and *Gcn2*$^{-/-}$ mice assessed by immunoblotting. *Left*, representative picture; *right*, quantitative analysis of the ApoB100 band. Data are mean ± S.D. *, $p < 0.05$ as compared with respective PBS control (*panels A*, *C*, *E*, and *F*) or lean counterparts *panel B*).

Asparaginase exposure decreased hepatic glutathione levels (supplemental Fig. S2*D*) similarly in both strains, reflecting a compromised ability to mount antioxidant defenses. On the other hand, *Gadd34* (*Ppp1r15*), a gene encoding an eIF2 phosphatase that functions as a negative regulator of ISR, was not induced by asparaginase in either strain (Fig. 2*C*), an effect possibly related to the reported influence of obesity on reducing GADD34 abundance (19). Furthermore, caspase-3 cleavage was also not increased by asparaginase in either strain (Fig. 2*D*), consistent with our previous findings in lean mice (6).

GCN2 is required for mTORC1 down-regulation in livers of asparaginase-treated obese mice

Our lab was the first to identify hyperactivation of mTORC1 during amino acid deprivation in *Gcn2*$^{-/-}$ conditions (14, 20). Genetic overactivation of hepatic mTORC1 reduces hydrogen

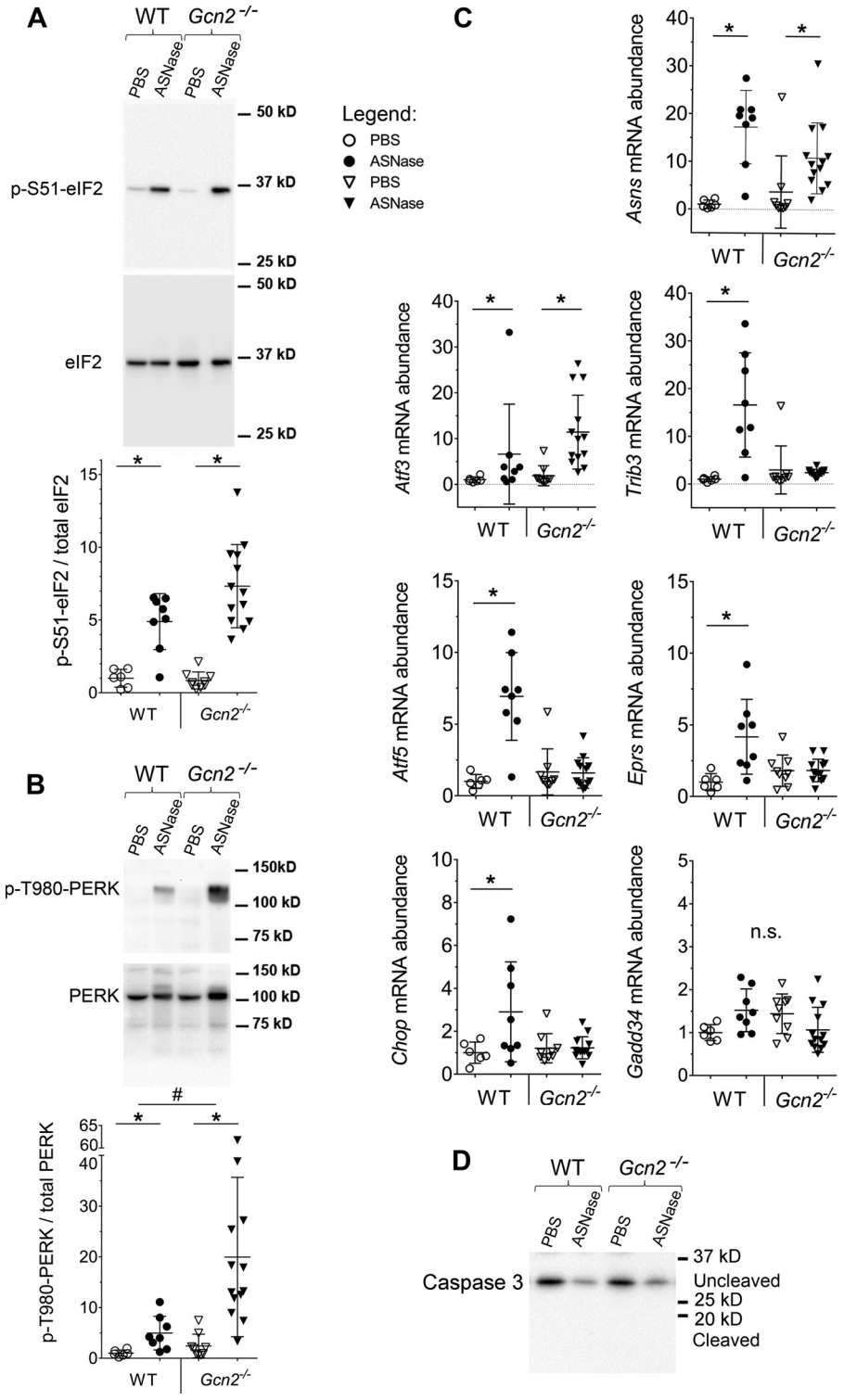

Figure 2. Activation of the ISR in the liver of WT and *Gcn2*$^{-/-}$ obese mice treated with ASNase or PBS. *A,* phosphorylation of eIF2 by immunoblot. Quantitative analysis of the relative band intensities are indicated for *p*-(S51)-eIF2. *B,* phosphorylation of PERK by immunoblot. Quantitative analysis of the relative band intensities are indicated for *p*-(T980)-PERK. *C,* relative hepatic abundancies of ISR transcripts, evaluated by quantitative RT-PCR. *D,* representative immunoblot showing asparaginase to not increase caspase 3 cleavage in liver of obese mice. Data are mean ± S.D. *, $p < 0.05$ as compared with respective PBS control. # marks difference between strains ($p < 0.05$). *n.s.*, no significant differences.

sulfide (H_2S) producing activity, leading to severe pathologies (21). To determine whether the GCN2-eIF2-ATF4 cascade functions to down-regulate mTORC1 activity and maintain H_2S production in liver during asparaginase, phosphorylation levels of ribosomal S6 kinase 1 (S6K1) and eIF4E-binding protein 1 (4E-BP1) in WT mice were first assessed. In WT mice, asparaginase significantly reduced the phosphorylation state of both proteins, whereas *Gcn2*$^{-/-}$ livers showed hyperphosphorylation of S6K1 and 4E-BP1 (Fig. 3, *A* and *B*). In agreement with these findings, asparaginase also increased phosphorylation of

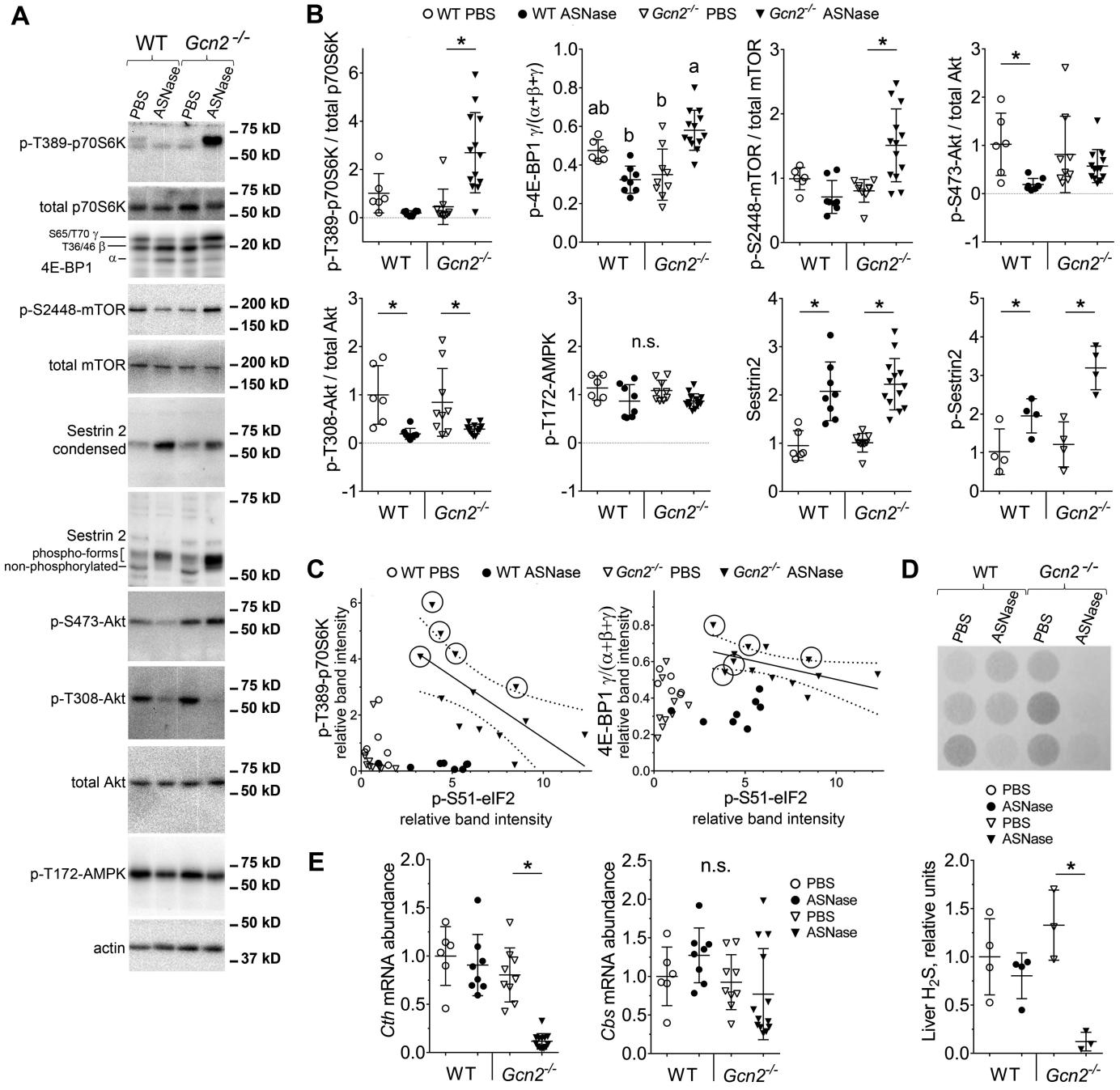

Figure 3. GCN2 deletion hyperactivates mTORC1 during ASNase treatment of obese mice. Representative images of immunoblots (*A*) and quantitative analysis of relative band intensities (*B*) for key components of mTORC1 pathway in the livers of WT and $Gcn2^{-/-}$ mice treated with ASNase or PBS. *C*, scatter plots of individual data points showing inverse relationships between *p*-(S51)-eIF2 and *p*-(T389)-S6K and between *p*-(S51)-eIF2 and γ-4E-BP1 in the $Gcn2^{-/-}$ ASNase-treated group. *Dotted lines* represent 95% confidence interval for Pearson's linear correlation analysis. *Circled* markers demarcate mice that became prematurely moribund. *D*, hepatic hydrogen sulfide production as measured by lead acetate method. *E*, quantitative analysis of *Cth* and *Cbs* gene expression evaluated by quantitative RT-PCR. Data are mean ± S.D. *, $p < 0.05$ as compared with respective PBS control. Means not sharing a letter are different according to Tukey post hoc when drug *X* strain interaction was revealed by analysis of variance. *n.s.*, no significant differences.

two downstream targets of S6K1, *p*-S2448-mTOR and *p*-S473-protein kinase B/Akt, in livers of $Gcn2^{-/-}$ as compared with WT mice (Fig. 3, *A* and *B*).

Further exploration into the relationship between the ISR and mTORC1 revealed that in the $Gcn2^{-/-}$ mice treated with asparaginase the levels of *p*-eIF2 correlated negatively with hyperphosphorylation of S6K1 (Pearson correlation coefficient, $r = -0.67$, $p < 0.01$) and 4E-BP1 (Pearson correlation coefficient for *p*-4EBP1 *versus p*-eIF2, $r = -0.55$, $p < 0.05$) (Fig. 3*C*). Furthermore, among the asparaginase-treated $Gcn2^{-/-}$ animals, the highest levels of mTORC1 activity corresponded with early onset of morbidity (*circled* points in Fig. 3*C*). Together, these data suggest that down-regulation of mTORC1 is a vital part of the liver adaptive response to asparaginase and is coordinated largely via GCN2.

Analysis of known upstream regulators of mTORC1 activity showed that activation of mTORC1 in the $Gcn2^{-/-}$ asparaginase-treated group was not due to increases in *p*-T308 Akt or

reductions in *p*-T172 AMP-activated protein kinase (AMPK) (Fig. 3, *A* and *B*). Levels of Sestrin2, an ATF4 target and inhibitor of mTORC1 activity during leucine deprivation (22), were also increased by asparaginase in both strains (Fig. 3, *A* and *B*). Next we analyzed the phosphorylation state of Sestrin2, which may also influence mTORC1 activity (23). Asparaginase caused hyperphosphorylation of Sestrin2 in WT and *Gcn2*$^{-/-}$ mice (Fig. 3, *A* and *B*), indicating that neither the expression nor phosphorylation of Sestrin2 is sufficient to inhibit mTORC1 upon these stress conditions *in vivo*. These results suggest that GCN2 serves as an essential component required to inhibit hepatic mTORC1 during asparaginase exposure independent of known upstream regulators, Akt, AMPK, and Sestrin2.

Finally, maladaptive activation of PERK and mTORC1 in obese *Gcn2*$^{-/-}$ mice treated with asparaginase coincided with reduced endogenous hydrogen sulfide (H_2S) production (Fig. 3*D*) and reduced mRNA levels of the ATF4 target gene, cystathionase/cystathionine γ-lyase (*Cth*), a key H_2S producing enzyme in the transsulfuration pathway (Fig. 3*E*). No correlation between hydrogen sulfide production and mRNA levels of another enzyme in the transsulfuration pathway, cystathionine β-synthase (*Cbs*), was observed (Fig. 3*E*). Furthermore, *p*-eIF2 by PERK was not sufficient to rescue H_2S production, suggesting a specific role for GCN2 rather than eIF2 phosphorylation *per se*.

Loss of hepatic Atf4 in combination with asparaginase does not reduce apolipoprotein B100

Phosphorylation of eIF2 promotes ATF4 synthesis, a key event driving ISR activation. To address the role of ATF4 following increased *p*-eIF2 by asparaginase, mice with genetic ablation of hepatic *Atf4* expression (*AlbCre Atf4*$^{f/f}$) and their congenic wild type Cre-negative counterparts (*Atf4*$^{f/f}$) were fed an obesogenic diet. Analyses of body composition during a 12-week feeding of the obesogenic diet revealed that both male and female *AlbCre Atf4*$^{f/f}$ mice maintained lean mass and were resistant to fat accumulation (Fig. 4*A*, and supplemental Fig. S3, *A* and *B*) despite consuming more food than their wild type counterparts (supplemental Fig. S3*C*). Thus, hepatic ATF4 plays an important role in whole body lipid metabolism, deposition, and storage. Assessment of glucose metabolism showed that genetic ablation of hepatic *Atf4* either directly or indirectly (via resistance to the fat gain) delayed the onset of glucose intolerance in males (Fig. 4*B*). Females of both strains were resistant to glucose intolerance development as in the previous cohort of mice (Fig. 4*B*).

Asparaginase proved catabolic in all diet-induced obese mice as evidenced by similar losses in body weight, body fat, and lean mass (Fig. 4*C*, and supplemental Fig. S4, *A* and *B*). In contrast to the *Gcn2*$^{-/-}$ animals, none of the asparaginase-treated *AlbCre Atf4*$^{f/f}$ mice displayed any signs of premature morbidity. Liver appearance and size relative to body weight, reduction in hepatic glutathione levels, and lipid accumulation in *Atf4*$^{f/f}$ and *AlbCre Atf4*$^{f/f}$ mice were similar to the first cohort of WT mice (Fig. 4, *D* and *E*, and supplemental Fig. S4, *C* and *D*). No disappearance of apolipoprotein B was observed in asparaginase-treated *AlbCre Atf4*$^{f/f}$ livers (Fig. 4*F*), indicating that maintenance of ApoB100 during asparaginase in liver requires GCN2 but not ATF4. Sexual dimorphism was not observed in the whole body response to chronic asparaginase exposure and so once again males and females were analyzed together in subsequent analyses.

Genetic ablation of hepatic Atf4 does not block asparaginase-induced ISR

Lean *AlbCre Atf4*$^{f/f}$ mice were previously characterized in studies aimed to investigate the role of ATF4 in chemically-induced ER stress (24). Analysis of obese *Atf4*$^{f/f}$ and *AlbCre Atf4*$^{f/f}$ animals for activation of the hepatic ISR to asparaginase showed similar induction of *p*-eIF2 (Fig. 5*A*), and *p*-PERK (Fig. 5*B*) in contrast to the larger increases observed in livers of *Gcn2*$^{-/-}$ mice.

Despite similar eIF2 phosphorylation levels to asparaginase, *AlbCre Atf4*$^{f/f}$ livers demonstrated substantial, albeit variable, changes in gene expression. For example, mRNA levels of *Chop*, *Atf3*, and *Trib3* increased tremendously (37-, 67-, and 120-fold, respectively) as compared with *Atf4*$^{f/f}$ wild type group (Fig. 5*C*) or the first experimental cohort of mice (Fig. 2, and). Analyses of *Chop*, *Atf3*, and *Trib3* mRNA induction in the *AlbCre Atf4*$^{f/f}$ asparaginase-treated group revealed strong positive correlations between the mRNA abundancies (Fig. 5*D*). Taken together, these data suggest that ATF4 functions to limit expression of these genes during asparaginase treatment. Furthermore, asparaginase-induced changes in *Atf5*, *Asns*, and *Eprs* transcript abundance were unaffected by loss of ATF4 (Fig. 5*C*), suggesting that transcriptional induction of many ISR target genes can be driven by an auxiliary factor(s) other than ATF4. Again, no changes in *Gadd34* expression were observed in livers from asparaginase-treated obese mice (Fig. 5*C*), supporting the idea that induction of *Gadd34* is impeded by obesity (19).

ATF4 is necessary for hydrogen sulfide production but not down-regulation of mTORC1 by asparaginase

Assessment of H_2S production showed that asparaginase exposure reduced H_2S production capacity (Fig. 6*A*). Loss of hepatic *Atf4* also reduced overall H_2S levels, in agreement with studies reporting that *Cth* is a target gene of ATF4 (25). Moreover hepatic capacity to produce H_2S correlated with the expression of *Cth* and not *Cbs* mRNA (Fig. 6*B*). Thus, the failure to maintain H_2S production in the liver of asparaginase-treated *Gcn2*$^{-/-}$ mice is due in part to reduced ATF4-driven gene expression. In contrast, assessment of mTORC1 signaling in obese *Atf4*$^{f/f}$ and *AlbCre Atf4*$^{f/f}$ mice revealed similar reductions in the levels of phosphorylated 4E-BP1, S6K1 (Thr-389), mTOR (Ser-2448), and Akt (Ser-473) upon asparaginase (Fig. 6, *C* and *D*). Analysis of upstream regulators of mTORC1 activity showed decreased phosphorylation of Akt (Thr-308) upon asparaginase, whereas AMPK phosphorylation remained stable (Fig. 6, *C* and *D*). Expression and phosphorylation of Sestrin2 was increased by asparaginase in both strains (Fig. 6, *C* and *D*). Taken together, these results suggest that asparaginase reduces mTORC1 independent of ATF4.

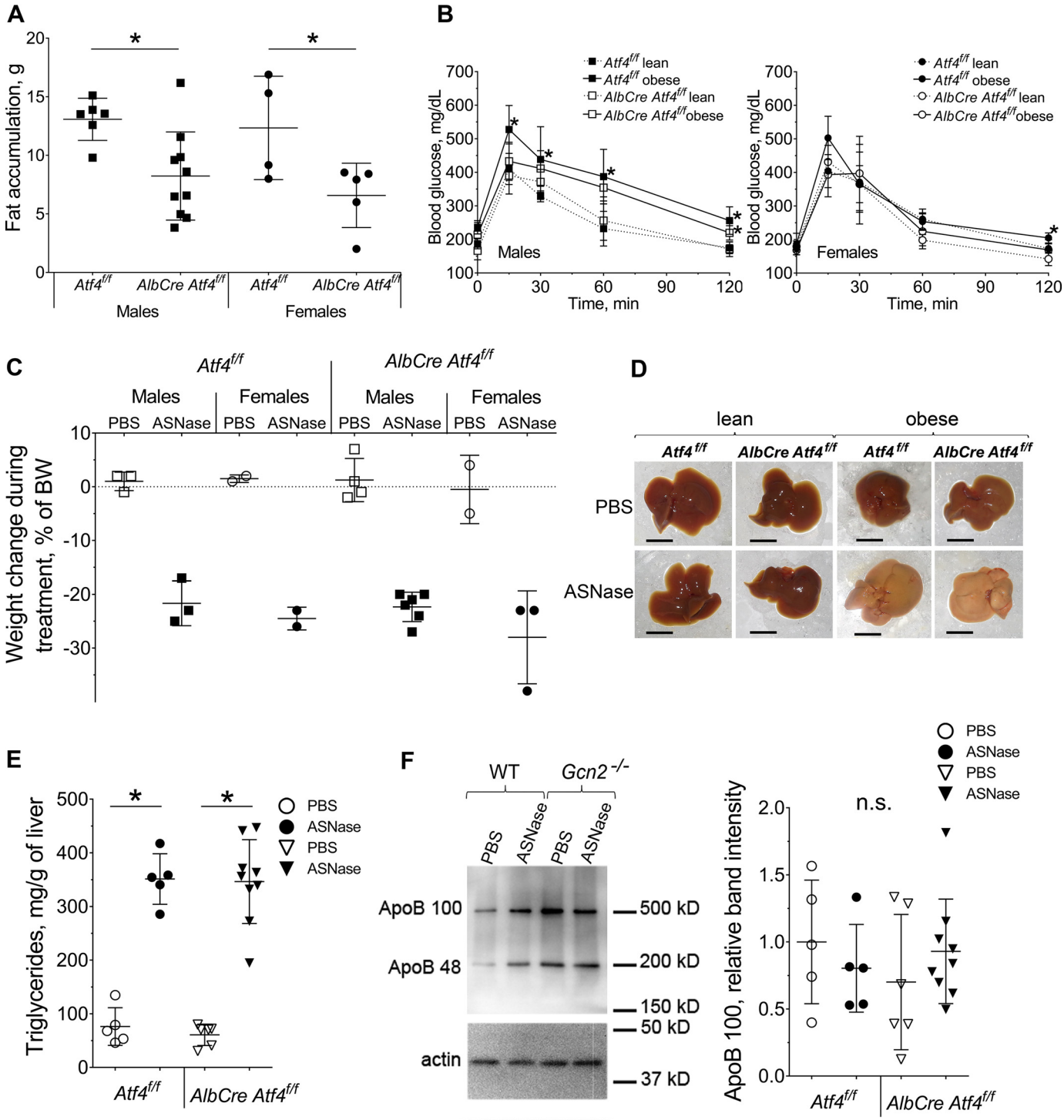

Figure 4. ASNase treatment promotes liver steatosis in obese wild type mice (*Atf4*$^{f/f}$) and mice deleted for hepatic *Atf4* (*AlbCre Atf4*$^{f/f}$). *A,* body fat accumulation in male and female mice after 12 weeks of an obesogenic diet, assessed by magnetic resonance imaging. *B,* glucose clearance in male and female mice after 12 weeks of an obesogenic diet. *C,* total body weight loss after 8 days of ASNase or PBS. *D,* gross morphology of livers from lean and obese mice after 8 days of ASNase or PBS. *Scale bar* is 1 cm. *E,* triglyceride accumulation in livers of obese animals. *F,* hepatic ApoB protein abundance was assessed by immunoblotting. *Left*, representative picture; *right*, quantitative analysis of the ApoB100 band. Data are mean ± S.D. *, $p < 0.05$ as compared with respective PBS control. *n.s.*, no significant differences.

Discussion

Maladaptive activation of the ISR and deregulation of the mTORC1 pathway are associated with obesity, hepatic insulin resistance, and ectopic fat deposition (26–28). Our findings demonstrate that diet-induced obesity challenges the hepatoprotective capacity of the ISR to amino acid depletion by asparaginase. Moreover, GCN2, the first responder to amino acid depletion, is required to prevent hyperactivation of mTORC1, maintain endogenous hydrogen sulfide production, and maintain hepatic expression of ApoB100 during asparaginase treat-

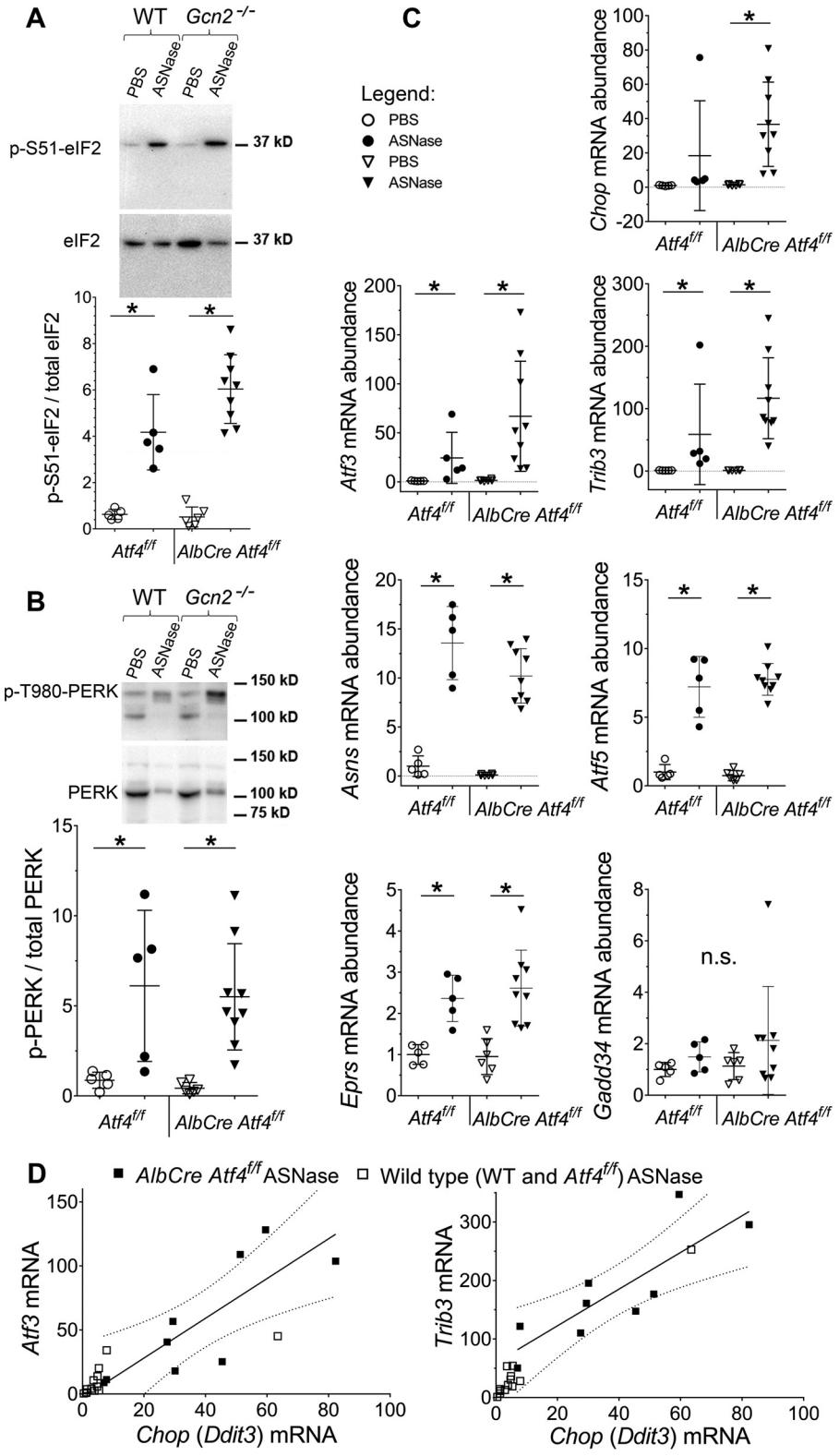

Figure 5. Activation of the ISR in mice deleted for *Atf4* in liver. *A,* phosphorylation of eIF2 by immunoblot. Representative image and quantitative analysis of the relative band intensities are indicated for *p*-(S51)-eIF2. *B,* phosphorylation of PERK by immunoblot. Representative image and quantitative analysis of relative band intensities are indicated for *p*-(T980)-PERK. *C,* relative abundances of ISR transcripts in livers of obese mice. *D,* scatter plot showing positive correlation between *Chop* and either *Atf3 or Trib3*. *Dotted lines* represent 95% confidence interval for Pearson's linear correlation analysis performed on *AlbCre Atf4$^{f/f}$* ASNase-treated group: *Atf3 versus Chop*, $r = 0.81$, $p < 0.05$, and *Trib3 versus Chop*, $r = 0.83$, $p < 0.05$. Data are mean ± S.D. *, $p < 0.05$ as compared with respective PBS control (*panels A* and *E*) or lean counterparts (*panel B*). *n.s.*, no significant differences.

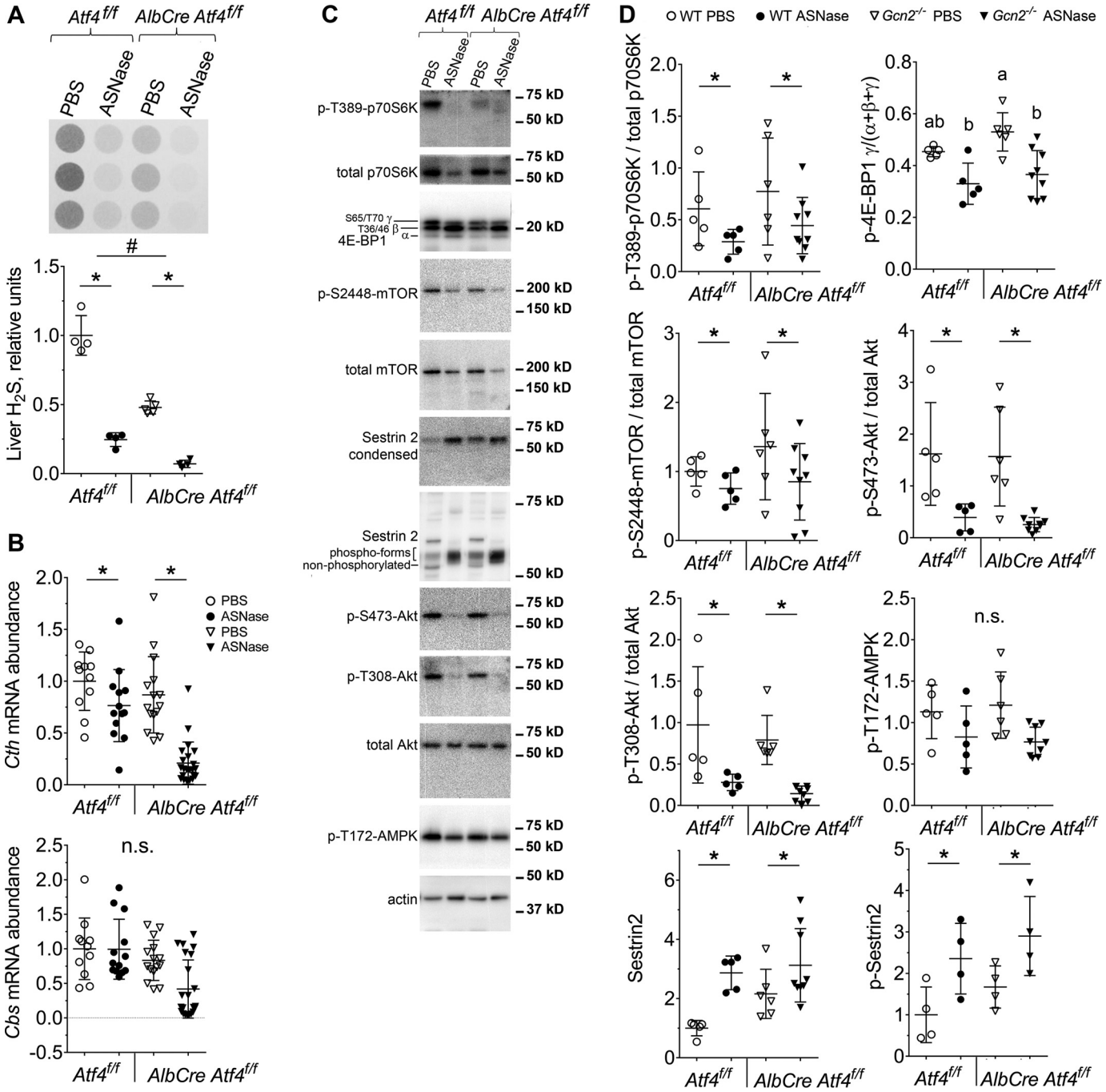

Figure 6. Genetic ablation of hepatic ATF4 fails to stimulate mTORC1 signaling during ASNase treatment. *A,* hepatic H_2S production as measured by lead acetate method. *B,* quantitative analysis of *Cth* and *Cbs* gene expression, assessed using quantitative RT-PCR. *C* and *D,* immunoblot analysis for key components of mTORC1 pathway: representative images (*C*) and quantitative analysis of relative band intensities (*D*). Data are represented as mean ± S.D. *, $p < 0.05$ as compared with respective PBS control. # marks difference between strains ($p < 0.05$). Means *not sharing a letter* are different according to Tukey post hoc when drug x strain interaction was revealed by ANOVA. *n.s.*, no significant differences.

ment. Compensatory activation of PERK fails to provide for these homeostatic responses in the absence of GCN2. Our study illuminates how a preexisting metabolic state, in combination with genetic background, guides hepatic adaptive responses to the amino acid deprivation induced by asparaginase.

Distinct outcomes following activation of the ISR by asparaginase in obese wild type and *Gcn2*$^{-/-}$ animals emphasize that each eIF2 kinase elicits distinct cellular response programs in addition to their shared ability to phosphorylate eIF2. One of the unique functions attributed to GCN2 is inhibition of mTORC1 activity during various states of amino acid deprivation (14, 20, 29, 30). Herein we report that in response to asparaginase treatment, GCN2 specifically inhibits hepatic mTORC1 by a mechanism independent of ATF4. This finding is consistent with a recent study of leucine deprivation in mouse embryonic fibroblasts (30) demonstrating that GCN2 rapidly inhibits mTORC1 via

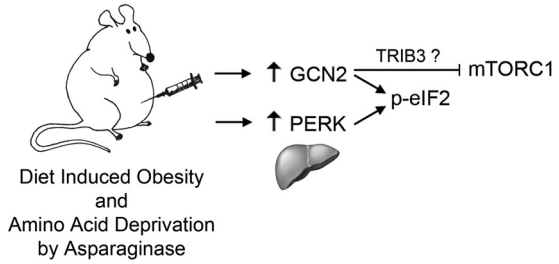

Figure 7. Model depicting molecular signaling during asparaginase treatment in obese animals. Under conditions of amino acid deprivation, GCN2 inhibits mTORC1-driven anabolic processes independently of phosphorylation of eIF2.

mechanism(s) requiring phosphorylation of eIF2. Extending these findings, our study demonstrates that the phosphorylation of eIF2 is not sufficient to rescue mTORC1 inhibition in the absence of GCN2. Thus, inhibition of mTORC1 during asparaginase is a unique function of GCN2, distinct from other eIF2 kinases (Fig. 7).

Exactly how loss of GCN2 unleashes mTORC1 activity during asparaginase remains uncertain. Previous reports in combination with the present findings show that GCN2-mediated mTORC1 repression is independent of several known upstream regulators of mTORC1 activity, namely REDD1, Akt, and AMPK (11, 14). ATF4-driven negative control of the mTORC1 pathway during leucine and glutamine deprivation reportedly occurs via Sestrin2 (22), forming the basis for our exploration in the current study. However, our findings show no relationship between *Atf4* expression and Sestrin2 protein levels or its phosphorylation status. Instead, our data suggest that the pseudokinase TRIB3 may be involved because loss of *Gcn2* but not *Atf4* blocked hepatic induction of *Trib3* by asparaginase. Studies in cells show TRIB3 to associate with Akt and suppress the Akt/mTOR axis, and knocking down Trib3 potentiates Akt Ser-473 phosphorylation by growth factors (31–33). In the current study, asparaginase inhibited Akt Ser-473 phosphorylation in wild type, $Atf4^{f/f}$, and *AlbCre* $Atf4^{f/f}$ mice but not $Gcn2^{-/-}$ mice. Thus, loss of TRIB3 induction may allow for dysregulation of the Akt/mTORC1 axis upon asparaginase. Future studies aimed to directly examine the role of TRIB3 in regulating mTORC1 signaling during asparaginase are warranted.

The capacity of the liver to produce hydrogen sulfide and maintain glutathione levels are essential for the organ health (34, 35). In our diet-induced obesity model, loss of *Gcn2* or *Atf4* maximally reduced endogenous hydrogen sulfide production during chronic asparaginase treatment. Hydrogen sulfide production correlates closely with the expression of *Cth*, an ATF4 target gene. Physiological role of hydrogen sulfide production during chronic ER stress has been studied in mouse embryonic fibroblast cell culture models utilizing thapsigargin, a chemical inducer of ER stress (36). The study reports that hydrogen sulfide production is triggered by chronic ER stress and leads to specific covalent modification (sulfhydration) of a number of metabolic enzymes to promote switching of cellular metabolism from oxidative phosphorylation to glycolysis. In the current study, we do not see increases in hydrogen sulfide production upon asparaginase exposure despite PERK activation in all strains. We interpret these findings to mean that endogenous production in liver during asparaginase requires the GCN2-eIF2-ATF4 axis, in line with the findings by others (10, 35). The combination of reduced H_2S capacity of liver during asparaginase when combined with hyperactivation of mTORC1, a known instigator of mitochondria function (37, 38), may result in an energy crisis and metabolic catastrophe, outcomes consistent with premature morbidity in $Gcn2^{-/-}$ mice.

Asparaginase is one in a growing class of GCN2-activating drugs (39–47). Our study identifies metabolic state as an important determinant of hepatoprotection during ISR activation by amino acid depletion. Furthermore, we identify GCN2 as a master regulator of mTORC1 that acts in an ATF4- and Sestrin2-independent manner. Moreover, our study demonstrates that genetic deletion of hepatic *Atf4* does not abolish expression of known ATF4 target genes, namely *Trib3, Chop,* and *Atf3*. Instead, these genes were induced to unprecedented levels, implying that ATF4 acts as a molecular rheostat, self-limiting the intensity of the ISR. This study provides novel information to help prevent or mitigate asparaginase-induced hepatotoxicity and will assist in the development of metabolic precision medicine (48).

Experimental procedures

Animals

All animals received humane care according to the criteria outlined in the "Guide for the Care and Use of Laboratory Animals" prepared by the National Academy of Sciences and published by the National Institute of Health (NIH publication 86–23 revised 1985) and ARRIVE (articulated at www.nc3rs.org.uk/ARRIVE). Animal protocols were reviewed and approved by The Rutgers Institutional Animal Care and Use Committee. Adult (10–20 weeks old) C57Bl/6J wild type (WT), $Gcn2^{-/-}$ (49), $Atf4^{f/f}$, and *AlbCre* $Atf4^{f/f}$ mice of both sexes were provided free access to food (5001 Laboratory Rodent Diet, LabDiet) and water and maintained on a 12-h light-dark cycle (7 a.m./7 p.m.) with same sex littermates until the experimental group assignment wherein mice were housed in individual plastic cages. Cages contained soft bedding and enrichment. The $Atf4^{f/f}$ strain was generated as described in Ref. 50 with loxP sites flanking the second and third exons of *Atf4* gene. The *AlbCre* $Atf4^{f/f}$ strain was generated by mating $Atf4^{f/f}$ mice to the mice bearing Cre-recombinase under albumin promoter allowing for liver-specific excision of the loxP flanked region in the offspring. All strains were on C57Bl/6J background for 8–10 generations.

Diet-induced obesity and assessment of glucose tolerance

All animals were fed a high-fat diet (20% protein, 20% carbohydrate, 60% fat/mostly lard; Research Diets Inc., D12492, NJ) *ad libitum* for 15 weeks. Food intake and body weight were monitored twice a week. Body composition was assessed by magnetic resonance imaging. At week 12, blood glucose was measured in conscious animals fasted for 6 h (8:30 am until 2:30 pm) in wire-bottom cages with free access to water. Glucose was administered orally by gavaging 20% glucose solution in the amount of 2 g/kg of lean mass; blood glucose concentration was measured 15, 30, 60, and 120 min following gavage.

Injections and sample collection

After 15 weeks of feeding obesogenic diets, animals were assigned to eight daily (9:00 am) intraperitoneal injections of either asparaginase (3 IU/g body weight, Elspar, Merck) or PBS excipient. Treatment assignment was based on total fat accumulation and glucose tolerance so that treatment groups were similar in this regard. Animals were killed by decapitation ~8 h following the final injection. Whole organs were rapidly dissected, weighed, and frozen in liquid nitrogen.

Liver triglycerides

Triglycerides were measured as described in Ref. 51 with minor modifications. Briefly, 20–30 mg of the frozen tissue powder was mixed with 0.4 ml of 1× PBS, 10 mM EDTA buffer. The resulting mixture was transferred to a screw cap glass tube containing 2 ml of hexane:isopropyl alcohol (1:4) solvent and incubated at room temperature for 10 min with periodic vortexing. Then 0.5 ml of hexane:diethyl ether (1:1) solvent was added to the glass tubes and the samples were incubated at room temperature for another 10 min with periodic vortexing. Then the samples were centrifuged (1,000–2,000 × *g* for 1 min) to facilitate phase separation and collect tissue debris at the bottom of the tube. Upper organic phase containing all the triglycerides extract from the tissue was transferred to a fresh screw cap glass tube and used to measure the amount of the triglycerides. Specifically, aliquots of the organic phase were first dried in the Savant SpeedVac concentrator equipped with a vapor trap and then assayed using Infinity TG reagent (Thermo Scientific number TR22421). Triglyceride amounts were calculated and reported as mg/g of tissue. Standard curve was generated using corn oil with the assumption that it has density of 0.92 g/cm^3. The corn oil was dissolved in hexane:isopropyl alcohol (4:1) solvent. Aliquots containing the amount of corn oil that are within the sensitivity range of the Infinity TG reagent were transferred to glass tubes, dried, and assayed in the same manner as the samples.

Hydrogen sulfide measurement

Hydrogen sulfide production was detected by lead acetate method (35). Briefly, 50 mg of flash frozen livers were homogenized in Passive Lysis Buffer (Promega). The lysates were freeze/thawed three times to facilitate homogenization and subsequently cleared by centrifugation. Protein concentrations were determined via bicinchoninic acid assay (Thermo Scientific). The hydrogen sulfide production reaction was set up in a 96-well plate by combining 100 μl of a reaction buffer (1× PBS supplemented with 10 mM L-cysteine and 1 mM pyridoxal 5′-phosphate) with 20 μl of the liver lysate, containing 5 μg of protein/μl in each well. A piece of lead acetate paper was secured on top of the 96-well plate with a 0.5-kg block weight. The reaction was carried out at 37 °C for 1 h. Detection of hydrogen sulfide was performed by quantification of dark spots of lead sulfide that formed on the paper during the reaction time. Densitometry was carried out using ImageJ software.

Hepatic glutathione measurement

Hepatic glutathione was measured in frozen powdered livers and Bioxytech GSH/GSSG-412 kit for colorimetric determination of reduced and oxidized glutathione (Percipio Biosciences number 21040) according to the manufacturer's instructions.

Quantitative RT-PCR analysis

RNA was isolated from 20 mg of frozen tissue powder using TRI Reagent according to the manufacturer instructions. Quality of the isolated RNA was assessed by measuring $A_{260/280}$ and $A_{260/230}$ ratios; integrity was assessed by visualization of the rRNA on agarose gel. One microgram of the isolated RNA from each sample was used to generate cDNA using High-Capacity cDNA Reverse Transcription Kit (Thermo Fisher, 4368814). The resulting cDNA was used for quantitative analysis of gene expression using the SYBR Green system. Primers used in this work are the following: *Asns* (forward, 5′-CTGTTACAATGGTGAAATCTACAACCACAAG-3′ and reverse, 5′-GATGAATGCAAACACCCCGTCCAGCATACAGAT-3′); *Ddit3/Chop* (forward, 5′-GAAGCCTGGTATGAGGATCTGCAGGAGGTC-3′ and reverse, 5′-CTTTGGGATGTGCGTGTGACCTCTGTTG-3′); *Ppp1r15a*/*Gadd34* (forward, 5′-CTTCGACTGCAGAGGCGGCTCAGATTG-3′ and reverse, 5′-GAAATGGACTGTGACTTTCTCAGCGAAGTGTAC-3′); *Atf3* (forward, 5′-CTGGAGATGTCAGTCACCAAGTCTGAG-3′ and reverse, 5′-CTCCAGTTTCTCTGACTCTTTCTGCAGGCAC-3′); *Eprs* (forward, 5′-TGTGGGGAAATTGACTGTGA-3′ and reverse, 5′-AACTCCGACCAAACAAGGTG-3′) gene expression. *Gapdh* (forward, 5′-GACAACTCACTCAAGATTGTCAGCAATGC-3′ and reverse, 5′-GTGGCAGTGATGGCATGGACTGTGGTC-3′) gene expression was used to normalize SYBR Green measured mRNA amounts. TaqMan probes were used to measure transcript abundancies *of Atf5* (Mm04179654_m1), *Cth* (Mm00461247_m1), and *Cbs* (Mm00460654_m1) genes.

Immunoblot analysis

Liver tissue was crushed using the Cellcrusher tissue pulverizer under liquid nitrogen conditions. Resulting tissue powder was lysed with RIPA buffer (25 mM HEPES, pH 7.5, 10 mM DTT, 0.1% SDS, 1× protease inhibitor mixture (Sigma), 1 mM sodium orthovanadate, 0.5% deoxycholate, 50 mM β-glycerophosphate, 2 mM EDTA, 1 mM microcystin, 50 mM NaF, 3 mM benzamidine) using the Polytron benchtop homogenizer followed by heating the lysates for 5 min in Laemmli buffer. Apolipoprotein B was resolved on 3–20% gradient gel, Sestrin2 phosphorylation was analyzed using 7.5% gel as described in Ref. 23. Primary antibodies used were: anti-total p70S6K (CST 9202), anti-p-(T389)-S6K (CST 9205), and anti-4E-BP1 (Bethyl Laboratories, A300–501A), anti-p-(s2448)-mTOR (CST 2971), anti-mTOR (CST 2972), anti-p-(S51)-eIF2 (CST 3597), anti-eIF2 (sc-11386), anti-p-(T308)-Akt (CST 9275), anti-p-(S473)-Akt (CST 9271), anti-Akt (CST 9272), anti-p-(T172)-AMPK (CST 2535), anti-Caspase 3 (CST 9662). Secondary antibody was peroxidase AffiniPure goat anti-rabbit TgC (H+L) from Jackson ImmunoResearch (111-035-003). Images were taken with Fluorchem M imager (ProteinSimple), band densities were quantified using AlphaView software.

Author contributions—Conception and design of the study was by I. A. N., R. C. W., and T. G. A.; generation, collection, assembly, analysis, and/or interpretation of data was by I. A. N., R. J. T. A., E. T. M., Y. W., M. P. G., B. B. W., J. L. D., C. H., J. R. M., C. M. A., R. C. W., and T. G. A.; drafting or revision of the manuscript by I. A. N., C. H., J. R. M., C. M. A., R. C. W., and T. G. A.; and approval of the final version of the manuscript was by I. A. N., R. J. T. A., E. T. M., Y. W., M. P. G., B. B. W., J. L. D., C. H., J. R. M., C. M. A., R. C. W., and T. G. A.

Acknowledgments—We thank Ashley Pettit for discussions throughout this work and Matthew Solowsky for technical assistance.

References

1. Inaba, H., Greaves, M., and Mullighan, C. G. (2013) Acute lymphoblastic leukaemia. *Lancet* **381,** 1943–1955
2. Bodmer, M., Sulz, M., Stadlmann, S., Droll, A., Terracciano, L., and Krähenbühl, S. (2006) Fatal liver failure in an adult patient with acute lymphoblastic leukemia following treatment with L-asparaginase. *Digestion* **74,** 28–32
3. Sahoo, S., and Hart, J. (2003) Histopathological features of L-asparaginase-induced liver disease. *Semin. Liver Dis.* **23,** 295–299
4. Orgel, E., Sposto, R., Malvar, J., Seibel, N. L., Ladas, E., Gaynon, P. S., and Freyer, D. R. (2014) Impact on survival and toxicity by duration of weight extremes during treatment for pediatric acute lymphoblastic leukemia: a report from the Children's Oncology Group. *J. Clin. Oncol.* **32,** 1331–1337
5. Reinert, R. B., Oberle, L. M., Wek, S. A., Bunpo, P., Wang, X. P., Mileva, I., Goodwin, L. O., Aldrich, C. J., Durden, D. L., McNurlan, M. A., Wek, R. C., and Anthony, T. G. (2006) Role of glutamine depletion in directing tissue-specific nutrient stress responses to L-asparaginase. *J. Biol. Chem.* **281,** 31222–31233
6. Wilson, G. J., Bunpo, P., Cundiff, J. K., Wek, R. C., and Anthony, T. G. (2013) The eukaryotic initiation factor 2 kinase GCN2 protects against hepatotoxicity during asparaginase treatment. *Am. J. Physiol. Endocrinol. Metab.* **305,** E1124–33
7. Harding, H. P., Novoa, I., Zhang, Y., Zeng, H., Wek, R., Schapira, M., and Ron, D. (2000) Regulated translation initiation controls stress-induced gene expression in mammalian cells. *Mol. Cell* **6,** 1099–1108
8. Vinson, C. R., Hai, T., and Boyd, S. M. (1993) Dimerization specificity of the leucine zipper-containing bZIP motif on DNA binding: prediction and rational design. *Genes Dev.* **7,** 1047–1058
9. Han, J., Back, S. H., Hur, J., Lin, Y.-H., Gildersleeve, R., Shan, J., Yuan, C. L., Krokowski, D., Wang, S., Hatzoglou, M., Kilberg, M. S., Sartor, M. A., and Kaufman, R. J. (2013) ER-stress-induced transcriptional regulation increases protein synthesis leading to cell death. *Nat. Cell Biol.* **15,** 481–490
10. Sikalidis, A. K., Lee, J.-I., and Stipanuk, M. H. (2011) Gene expression and integrated stress response in HepG2/C3A cells cultured in amino acid deficient medium. *Amino Acids* **41,** 159–171
11. Wilson, G. J., Lennox, B. A., She, P., Mirek, E. T., Al Baghdadi, R. J., Fusakio, M. E., Dixon, J. L., Henderson, G. C., Wek, R. C., and Anthony, T. G. (2015) GCN2 is required to increase fibroblast growth factor 21 and maintain hepatic triglyceride homeostasis during asparaginase treatment. *Am. J. Physiol. Endocrinol. Metab.* **308,** E283–93
12. Phillipson-Weiner, L., Mirek, E. T., Wang, Y., McAuliffe, W. G., Wek, R. C., and Anthony, T. G. (2016) General control nonderepressible 2 deletion predisposes to asparaginase-associated pancreatitis in mice. *Am. J. Physiol. Gastrointest. Liver Physiol.* **310,** $G_1$061–70
13. Bunpo, P., Cundiff, J. K., Reinert, R. B., Wek, R. C., Aldrich, C. J., and Anthony, T. G. (2010) The eIF2 kinase GCN2 is essential for the murine immune system to adapt to amino acid deprivation by asparaginase. *J. Nutr.* **140,** 2020–2027
14. Bunpo, P., Dudley, A., Cundiff, J. K., Cavener, D. R., Wek, R. C., and Anthony, T. G. (2009) GCN2 protein kinase is required to activate amino acid deprivation responses in mice treated with the anti-cancer agent L-asparaginase. *J. Biol. Chem.* **284,** 32742–32749
15. Rousseau, J., Gagné, V., Labuda, M., Beaubois, C., Sinnett, D., Laverdière, C., Moghrabi, A., Sallan, S. E., Silverman, L. B., Neuberg, D., Kutok, J. L., and Krajinovic, M. (2011) ATF5 polymorphisms influence ATF function and response to treatment in children with childhood acute lymphoblastic leukemia. *Blood* **118,** 5883–5890
16. Ben Tanfous, M., Sharif-Askari, B., Ceppi, F., Laaribi, H., Gagné, V., Rousseau, J., Labuda, M., Silverman, L. B., Sallan, S. E., Neuberg, D., Kutok, J. L., Sinnett, D., Laverdière, C., and Krajinovic, M. (2015) Polymorphisms of asparaginase pathway and asparaginase-related complications in children with acute lymphoblastic leukemia. *Clin. Cancer Res.* **21,** 329–334
17. Harding, H. P., Zhang, Y., and Ron, D. (1999) Protein translation and folding are coupled by an endoplasmic reticulum-resident kinase. *Nature* **397,** 271–274
18. Dang Do, A. N., Kimball, S. R., Cavener, D. R., and Jefferson, L. S. (2009) eIF2α kinases GCN2 and PERK modulate transcription and translation of distinct sets of mRNAs in mouse liver. *Physiol. Genomics* **38,** 328–341
19. Rinella, M. E., Siddiqui, M. S., Gardikiotes, K., Gottstein, J., Elias, M., and Green, R. M. (2011) Dysregulation of the unfolded protein response in db/db mice with diet-induced steatohepatitis. *Hepatology* **54,** 1600–1609
20. Anthony, T. G., McDaniel, B. J., Byerley, R. L., McGrath, B. C., Cavener, D. R., McNurlan, M. A., and Wek, R. C. (2004) Preservation of liver protein synthesis during dietary leucine deprivation occurs at the expense of skeletal muscle mass in mice deleted for eIF2 kinase GCN2. *J. Biol. Chem.* **279,** 36553–36561
21. Menon, S., Yecies, J. L., Zhang, H. H., Howell, J. J., Nicholatos, J., Harputlugil, E., Bronson, R. T., Kwiatkowski, D. J., and Manning, B. D. (2012) Chronic activation of mTOR complex 1 is sufficient to cause hepatocellular carcinoma in mice. *Sci. Signal.* **5,** ra24
22. Ye, J., Palm, W., Peng, M., King, B., Lindsten, T., Li, M. O., Koumenis, C., and Thompson, C. B. (2015) GCN2 sustains mTORC1 suppression upon amino acid deprivation by inducing Sestrin2. *Genes Dev.* **29,** 2331–2336
23. Kimball, S. R., Gordon, B. S., Moyer, J. E., Dennis, M. D., and Jefferson, L. S. (2016) Leucine induced dephosphorylation of Sestrin2 promotes mTORC1 activation. *Cell. Signal* **28,** 896–906
24. Fusakio, M. E., Willy, J. A., Wang, Y., Mirek, E. T., Al Baghdadi, R. J., Adams, C. M., Anthony, T. G., and Wek, R. C. (2016) Transcription factor ATF4 directs basal and stress-induced gene expression in the unfolded protein response and cholesterol metabolism in the liver. *Mol. Biol. Cell.* **27,** 1536–1551
25. Dickhout, J. G., Carlisle, R. E., Jerome, D. E., Mohammed-Ali, Z., Jiang, H., Yang, G., Mani, S., Garg, S. K., Banerjee, R., Kaufman, R. J., Maclean, K. N., Wang, R., and Austin, R. C. (2012) Integrated stress response modulates cellular redox state via induction of cystathionine γ-lyase: cross-talk between integrated stress response and thiol metabolism. *J. Biol. Chem.* **287,** 7603–7614
26. Samuel, V. T., and Shulman, G. I. (2012) Mechanisms for insulin resistance: common threads and missing links. *Cell.* **148,** 852–871
27. Ozcan, U., Cao, Q., Yilmaz, E., Lee, A.-H., Iwakoshi, N. N., Ozdelen, E., Tuncman, G., Görgün, C., Glimcher, L. H., and Hotamisligil, G. S. (2004) Endoplasmic reticulum stress links obesity, insulin action, and type 2 diabetes. *Science* **306,** 457–461
28. Laplante, M., and Sabatini, D. M. (2012) mTOR signaling in growth control and disease. *Cell* **149,** 274–293
29. Xiao, F., Huang, Z., Li, H., Yu, J., Wang, C., Chen, S., Meng, Q., Cheng, Y., Gao, X., Li, J., Liu, Y., and Guo, F. (2011) Leucine deprivation increases hepatic insulin sensitivity via GCN2/mTOR/S6K1 and AMPK pathways. *Diabetes* **60,** 746–756
30. Averous, J., Lambert-Langlais, S., Mesclon, F., Carraro, V., Parry, L., Jousse, C., Bruhat, A., Maurin, A.-C., Pierre, P., Proud, C. G., and Fafournoux, P. (2016) GCN2 contributes to mTORC1 inhibition by leucine deprivation through an ATF4 independent mechanism. *Sci. Rep.* **6,** 27698
31. Erazo, T., Lorente, M., López-Plana, A., Muñoz-Guardiola, P., Fernández-Nogueira, P., García-Martínez, J. A., Bragado, P., Fuster, G., Salazar, M., Espadaler, J., Hernández-Losa, J., Bayascas, J. R., Cortal, M., Vidal, L., Gascón, P., *et al.* (2016) The new antitumor drug ABTL0812 inhibits the

Akt/mTORC1 axis by upregulating tribbles-3 pseudokinase. *Clin. Cancer Res.* **22,** 2508–2519
32. Salazar, M., Lorente, M., García-Taboada, E., Pérez Gómez, E., Dávila, D., Zúñiga-García, P., María Flores, J., Rodríguez, A., Hegedus, Z., Mosén-Ansorena, D., Aransay, A. M., Hernández-Tiedra, S., López-Valero, I., Quintanilla, M., Sánchez, C., *et al.* (2015) Loss of Tribbles pseudokinase-3 promotes Akt-driven tumorigenesis via FOXO inactivation. *Cell Death Differ.* **22,** 131–144
33. Du, K., Herzig, S., Kulkarni, R. N., and Montminy, M. (2003) TRB3: a tribbles homolog that inhibits Akt/PKB activation by insulin in liver. *Science* **300,** 1574–1577
34. Mani, S., Cao, W., Wu, L., and Wang, R. (2014) Hydrogen sulfide and the liver. *Nitric Oxide* **41,** 62–71
35. Hine, C., Harputlugil, E., Zhang, Y., Ruckenstuhl, C., Lee, B. C., Brace, L., Longchamp, A., Treviño-Villarreal, J. H., Mejia, P., Ozaki, C. K., Wang, R., Gladyshev, V. N., Madeo, F., Mair, W. B., and Mitchell, J. R. (2015) Endogenous hydrogen sulfide production is essential for dietary restriction benefits. *Cell.* **160,** 132–144
36. Gao, X.-H., Krokowski, D., Guan, B.-J., Bederman, I., Majumder, M., Parisien, M., Diatchenko, L., Kabil, O., Willard, B., Banerjee, R., Wang, B., Bebek, G., Evans, C. R., Fox, P. L., Gerson, S. L., *et al.* (2015) Quantitative H2S-mediated protein sulfhydration reveals metabolic reprogramming during the integrated stress response. *Elife* **4,** e10067
37. Morita, M., Gravel, S.-P., Chénard, V., Sikström, K., Zheng, L., Alain, T., Gandin, V., Avizonis, D., Arguello, M., Zakaria, C., McLaughlan, S., Nouet, Y., Pause, A., Pollak, M., Gottlieb, E., *et al.* (2013) mTORC1 controls mitochondrial activity and biogenesis through 4E-BP-dependent translational regulation. *Cell Metab.* **18,** 698–711
38. Ramanathan, A., and Schreiber, S. L. (2009) Direct control of mitochondrial function by mTOR. *Proc. Natl. Acad. Sci. U.S.A.* **106,** 22229–22232
39. Hernandez, C. P., Morrow, K., Lopez-Barcons, L. A., Zabaleta, J., Sierra, R., Velasco, C., Cole, J., and Rodriguez, P. C. (2010) Pegylated arginase I: a potential therapeutic approach in T-ALL. *Blood* **115,** 5214–5221
40. Morrow, K., Hernandez, C. P., Raber, P., Del Valle, L., Wilk, A. M., Majumdar, S., Wyczechowska, D., Reiss, K., and Rodriguez, P. C. (2013) Anti-leukemic mechanisms of pegylated arginase I in acute lymphoblastic T-cell leukemia. *Leukemia* **27,** 569–577
41. Patil, M. D., Bhaumik, J., Babykutty, S., Banerjee, U. C., and Fukumura, D. (2016) Arginine dependence of tumor cells: targeting a chink in cancer's armor. *Oncogene* **35,** 4957–4972
42. Yau, T., Cheng, P. N., Chan, P., Chan, W., Chen, L., Yuen, J., Pang, R., Fan, S. T., and Poon, R. T. (2013) A phase 1 dose-escalating study of pegylated recombinant human arginase 1 (Peg-rhArg1) in patients with advanced hepatocellular carcinoma. *Invest. New Drugs* **31,** 99–107
43. Ni, Y., Schwaneberg, U., and Sun, Z.-H. (2008) Arginine deiminase, a potential anti-tumor drug. *Cancer Lett.* **261,** 1–11
44. Keller, T. L., Zocco, D., Sundrud, M. S., Hendrick, M., Edenius, M., Yum, J., Kim, Y.-J., Lee, H.-K., Cortese, J. F., Wirth, D. F., Dignam, J. D., Rao, A., Yeo, C.-Y., Mazitschek, R., and Whitman, M. (2012) Halofuginone and other febrifugine derivatives inhibit prolyl-tRNA synthetase. *Nat. Chem. Biol.* **8,** 311–317
45. Zhou, H., Sun, L., Yang, X.-L., and Schimmel, P. (2013) ATP-directed capture of bioactive herbal-based medicine on human tRNA synthetase. *Nature* **494,** 121–124
46. Peng, W., Robertson, L., Gallinetti, J., Mejia, P., Vose, S., Charlip, A., Chu, T., and Mitchell, J. R. (2012) Surgical stress resistance induced by single amino acid deprivation requires Gcn2 in mice. *Sci. Transl. Med.* **4,** 118ra11
47. Sundrud, M. S., Koralov, S. B., Feuerer, M., Calado, D. P., Kozhaya, A. E., Rhule-Smith, A., Lefebvre, R. E., Unutmaz, D., Mazitschek, R., Waldner, H., Whitman, M., Keller, T., and Rao, A. (2009) Halofuginone inhibits TH17 cell differentiation by activating the amino acid starvation response. *Science* **324,** 1334–1338
48. Schork, N. J. (2015) Personalized medicine: time for one-person trials. *Nature* **520,** 609–611
49. Zhang, P., McGrath, B. C., Reinert, J., Olsen, D. S., Lei, L., Gill, S., Wek, S. A., Vattem, K. M., Wek, R. C., Kimball, S. R., Jefferson, L. S., and Cavener, D. R. (2002) The GCN2 eIF2α kinase is required for adaptation to amino acid deprivation in mice. *Mol. Cell. Biol.* **22,** 6681–6688
50. Ebert, S. M., Dyle, M. C., Kunkel, S. D., Bullard, S. A., Bongers, K. S., Fox, D. K., Dierdorff, J. M., Foster, E. D., and Adams, C. M. (2012) Stress-induced skeletal muscle Gadd45a expression reprograms myonuclei and causes muscle atrophy. *J. Biol. Chem.* **287,** 27290–27301
51. Schwartz, D. M., and Wolins, N. E. (2007) A simple and rapid method to assay triacylglycerol in cells and tissues. *J. Lipid Res.* **48,** 2514–2520